

PAPER

# X-ray absorption investigation of the site occupancies of the copper element in nominal $\text{Cu}_3\text{Zn}(\text{OH})_6\text{FBr}^*$

To cite this article: Ruitang Wang *et al* 2021 *Chinese Phys. B* **30** 046102

View the [article online](#) for updates and enhancements.

## You may also like

- [Characterization of OH species in kHz He/H<sub>2</sub>O atmospheric pressure dielectric barrier discharges](#)  
Jyun-Yu Lin, Cheng-Liang Huang, Jui-Wen Chen *et al.*
- [Synthesis of Zinc-Terephthalate Metal Organic Frameworks and Their Application to Redox Batteries](#)  
Satoshi Chubachi, Tensho Nakamura, Shotaro Ueda *et al.*
- [Ternary organic photodetectors based on pseudo-binaries nonfullerene-based acceptors](#)  
Tianyi Zhang, Maximilian Moser, Alberto D Scaccabarozzi *et al.*

# X-ray absorption investigation of the site occupancies of the copper element in nominal $\text{Cu}_3\text{Zn}(\text{OH})_6\text{FBr}^*$

Ruitang Wang(王瑞塘)<sup>1,2</sup>, Xiaoting Li(李效亭)<sup>3</sup>, Xin Han(韩鑫)<sup>1,2</sup>, Jiaqi Lin(林佳琪)<sup>1,2</sup>, Yong Wang(王勇)<sup>4</sup>, Tian Qian(钱天)<sup>1,5</sup>, Hong Ding(丁洪)<sup>1,5</sup>, Youguo Shi(石友国)<sup>1,2</sup>, and Xuerong Liu(柳学榕)<sup>3,†</sup>

<sup>1</sup>Beijing National Laboratory for Condensed Matter Physics and Institute of Physics, Chinese Academy of Sciences, Beijing 100190, China

<sup>2</sup>University of Chinese Academy of Sciences, Beijing 100049, China

<sup>3</sup>School of Physical Science and Technology, ShanghaiTech University, Shanghai 201210, China

<sup>4</sup>Shanghai Synchrotron Radiation Facility, Shanghai Institute of Applied Physics, Chinese Academy of Sciences, Shanghai 201800, China

<sup>5</sup>Songshan Lake Materials Laboratory, Dongguan 250100, China

(Received 30 December 2020; revised manuscript received 22 January 2021; accepted manuscript online 28 January 2021)

With Zn substitution to the three-dimensional antiferromagnetically ordered barlowite  $\text{Cu}_4(\text{OH})_6\text{FBr}$ ,  $\text{Cu}_3\text{Zn}(\text{OH})_6\text{FBr}$  shows no magnetic phase transition down to 50 mK, and the system is suggested to be a two-dimensional kagomé quantum spin liquid [*Chin. Phys. Lett.* **34** 077502 (2017)]. A key issue to identify such phase diagram is the exact chemical formula of the substituted compound. With Cu *L*-edge x-ray absorption spectrum (XAS) combined with the MultiX XAS calculations, we evaluate the Cu concentration in a nominal  $\text{Cu}_3\text{Zn}(\text{OH})_6\text{FBr}$  sample. Our results show that although the Cu concentration is 2.80, close to the expected value, there is 34% residual Cu occupation in intersite layers between kagomé layers. Thus the Zn substitution of the intersite layers is not complete, and likely it intrudes the kagomé layers.

**Keywords:** x-ray absorption spectrum, barlowite spin liquid candidate, chemical occupations

**PACS:** 61.05.cj, 75.10.Kt, 71.15.Mb, 61.50.Nw

**DOI:** 10.1088/1674-1056/abe0c8

## 1. Introduction

Quantum spin liquid (QSL) is a quantum state where the spins are long-range entangled but host no symmetry breaking.<sup>[2]</sup> With the spins being quantum coherent and arranged in a superposition state, QSL is predicted to have exotic properties.<sup>[3,4]</sup> Efforts to realize QSL state have been much focused on low dimensional geometrically spin frustrated systems,<sup>[5–8]</sup> such as two-dimensional kagomé lattice,<sup>[9]</sup> but so far the results are still elusive. The main challenge is that, since the QSL results from the delicate balance of the microscopic interactions with quantum fluctuations, such state is highly susceptible to perturbations, including non-intrinsic chemical imperfectness.

For example, herbertsmithite  $\text{ZnCu}_3(\text{OH})_6\text{Cl}_2$  has been experimentally suggested to show many QSL properties.<sup>[10–15]</sup> However, it is known that keeping the fine balancing for herbertsmithite  $\text{ZnCu}_3(\text{OH})_6\text{Cl}_2$  is tricky because of the imperfect alignment of kagomé planes<sup>[17]</sup> and possible lattice distortion due to the antisite disorder.<sup>[18,20]</sup> Nominally, the Cu is expected to occupy the kagomé planes while the Zn is expected to stay in the interlayer sites. In  $\text{ZnCu}_3(\text{OH})_6\text{Cl}_2$  samples which showed no magnetic order down to 20 mK,<sup>[11,12,22]</sup> inelastic neutron scattering (INS) results suggested spinon-like dispersionless magnetic excitations.<sup>[23,24]</sup> But later it was

found that the residual  $\text{Cu}^{2+}$  on the interlayer site contributes mostly to these low energy excitations.<sup>[11,24–27]</sup> With x-ray anomalous scattering, Freedman *et al.* suggested that intersite  $\text{Cu}^{2+}$  impurity concentration is about 15% in their nominal  $\text{ZnCu}_3(\text{OH})_6\text{Cl}_2$  sample.<sup>[20]</sup>

Recently, a new kagomé layered system, barlowite  $\text{Cu}_4(\text{OH})_6\text{FBr}$  and the end member of Zn-doped compound  $\text{Cu}_3\text{Zn}(\text{OH})_6\text{FBr}$  were synthesized and investigated, which will be referred as  $\text{Cu}_4$  and  $\text{Cu}_3$  respectively in the following text. They are of a hexagonal crystal structure ( $P6_3/mmc$ ) at room temperature,<sup>[1,28–30]</sup> as shown in Fig. 1. This family is also built from kagomé planes and interlayer planes, with their kagomé planes proposed to be perfectly arranged.<sup>[17]</sup> And with a different coordination environment (trigonal prismatic) around the interlayer  $\text{Cu}^{2+}$  site compared to herbertsmithite (octahedral), a lower amount of  $\text{Cu}^{2+}$  defects were predicted.<sup>[18,19]</sup>

Experimental results showed that, while  $\text{Cu}_4(\text{OH})_6\text{FBr}$  undergoes an antiferromagnetic (AF) transition at about 15 K,<sup>[26,28,31]</sup> no magnetic order is observed in  $\text{Cu}_3\text{Zn}(\text{OH})_6\text{FBr}$  down to 50 mK.<sup>[28]</sup> Further, susceptibility and specific heat studies as well as theoretical calculations<sup>[29]</sup> suggested that a robust QSL is realized in partially Zn-doped compounds, consistent with former results which indicated

\*Project supported by the National Natural Science Foundation of China (Grant Nos. 11934017 and 11774399), the Key Research and Development Program of China (Grant No. 2016YFA0401000), the Chinese Academy of Sciences (Grant No. 112111KYSB20170059), and the K. C. Wong Education Foundation (Grant No. GJTD-2018-01).

†Corresponding author. E-mail: liuxr@shanghaitech.edu.cn

© 2021 Chinese Physical Society and IOP Publishing Ltd

<http://iopscience.iop.org/cpb> <http://cpb.iphys.ac.cn>

that compounds with larger than 30% Zn replacement of the Cu in the interlayers may have intrinsic spin liquid kagomé planes.<sup>[28]</sup> All these studies rely on the assumption that the kagomé layer is perfect with full Cu occupation. Obviously, from the lessons we learned on the nominal  $\text{ZnCu}_3(\text{OH})_6\text{Cl}_2$ , a precise determination of the site occupations is critical in identifying QSL in real materials.

The inductively coupled plasma optical emission spectrometry (ICP-OES)<sup>[28,30]</sup> and the energy dispersive x-ray spectroscopy (EDS) are often used to determine the chemical ratio of a compound. But the former technique is site-insensitive, thus can not disentangle the interlayer from intra-plane impurities,<sup>[32]</sup> and the latter one often bears poor energy resolution for insulating materials and requires standards with similar composition, which limit the accuracy of this quantization.<sup>[33]</sup> Anomalous x-ray scattering has been used to site-selectively estimate the Cu and Zn occupations in herbertsmithite.<sup>[20,21]</sup> But the analysis depends on comparison to tabulated anomalous scattering factor calculated from the Hatree–Fock wave functions of atoms. These values may not be accurate enough since they depend on the particular chemical environments of the ions.<sup>[34]</sup>

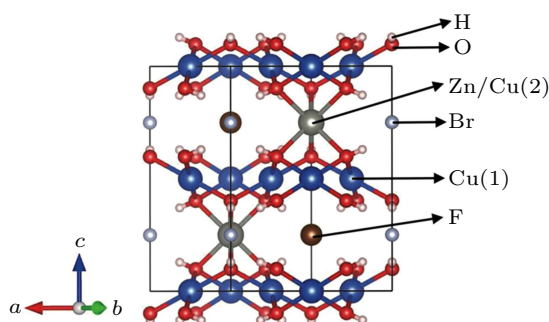


**Fig. 1.** Crystal structure of  $\text{Cu}_4(\text{OH})_6\text{FBr}$  ( $\text{Cu}_4$ ) and  $\text{Cu}_3\text{Zn}(\text{OH})_6\text{FBr}$  ( $\text{Cu}_3$ ). Both materials crystallize in  $P6_3/mmc$  space group at 300 K. In  $\text{Cu}_4(\text{OH})_6\text{FBr}$ ,  $\text{Cu}^{2+}$  ions lie on intra-kagomé plane site (Cu(1)) and inter-kagomé plane site (Cu(2)), respectively. Cu(1) has an octahedral ligand field while Cu(2) has a trigonal prismatic ligand field.

Here we use Cu  $L$ -edge x-ray absorption spectroscopy,<sup>[35]</sup> combined with the MultiX multiplet calculations,<sup>[36]</sup> to evaluate the contents of inter-layer and intra-plane  $\text{Cu}^{2+}$  in the nominal  $\text{Cu}_3\text{Zn}(\text{OH})_6\text{FBr}$ . Our results suggest that the metal sites in the kagomé planes are  $\sim 82\%$  occupied by Cu, while the interlayer metal sites are  $\sim 34\%$  occupied by Cu. Thus there is a strong antisite disorder, and likely the Zn substitution intrudes the kagomé planes. By assuming that the rest of the metal sites are all occupied by Zn without voids, we estimate the atomic ratio between Cu and Zn to be 1:0.43, close to the values we reported earlier from the EDS measurements.<sup>[1]</sup>

## 2. Experimental methods

Nominal  $\text{Cu}_4(\text{OH})_6\text{FBr}$  and  $\text{Cu}_3\text{Zn}(\text{OH})_6\text{FBr}$  powders were synthesized by the hydrothermal method.<sup>[28]</sup> The pow-

ders were pressed with 8 GPa pressure into dense tablets. After fine polishing, 50 nm platinum electric contact was deposited on the tablet surfaces by pulsed laser deposition (PLD) method, leaving the tablet center an open area for x-ray absorption spectroscopy (XAS) measurements. Both samples were prepared with the same processes under identical conditions. XAS measurements in total-electron-yield (TEY) mode near Cu  $L_3$  ( $2p_{3/2} \rightarrow 3d$ ) and  $L_2$  ( $2p_{1/2} \rightarrow 3d$ ) edges were performed at beamline BL08U1-A, Shanghai Synchrotron Radiation Facility (SSRF). Incoming x-ray beam was perpendicular to the sample surface. All measurements were carried out at 300 K.

## 3. Results

The main results are shown in Fig. 2. XAS spectra were normalized to the incident beam intensity. The two spectra from  $\text{Cu}_4$  and  $\text{Cu}_3$  are vertically stacked for clarity. In these measurements, the signal is sensitive to the unoccupied 3d states of the Cu element. The photoelectron absorption cross section can be written as<sup>[41]</sup>

$$\sigma \sim \rho(x) |\hat{M}_{if}|^2 \delta(E_f - E_i), \quad (1)$$

where  $\rho(x)$  is the density of the absorbing  $\text{Cu}^{2+}$  species, and  $\hat{M}_{if}$  is the photon absorption matrix element which can be reduced to the form  $\hat{M}_{if} = \langle f | \boldsymbol{\varepsilon} \cdot \boldsymbol{r} | i \rangle$  with dipole approximation.  $\delta(E_f - E_i)$  regulates the matching of the incident x-ray energy to the energy difference between the  $2p^6 3d^n$  ground states and the excited  $2p^5 3d^{n+1}$  states through photon absorption. Since the 2p states are split into the  $2p_{3/2}$  and  $2p_{1/2}$  manifolds due to strong core-level spin–orbit coupling, two major absorption peaks are observed (Fig. 2) which correspond to the so called  $L_3$  and  $L_2$  excitations.

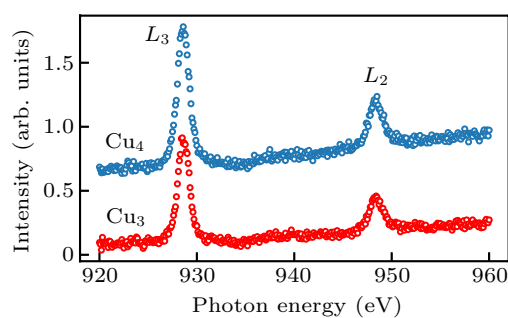


**Fig. 2.** X-ray absorption spectra of  $\text{Cu}_4$  and  $\text{Cu}_3$ . The measurements were carried out with total electron yield (TEY) mode. The spectra are vertically shifted for clarity.

As less Cu density is expected for the  $\text{Cu}_3$  sample, the reduced absorption strength is also expected as suggested by Eq. (1). The data shown in Fig. 2 agrees with such expectation. We will use this sensitivity to deduce the Cu concentration in our sample. It is interesting to notice that, although there are two non-equivalent Cu sites in the  $\text{Cu}_4$  sample, the spectral peaks are quite similar to those of the  $\text{Cu}_3$  sample. This observation indicates that the electronic configurations of the Cu(1)

and Cu(2) (Fig. 1) sites are quite close in energy, consistent with the DFT calculations.<sup>[17]</sup>

To extract the spectral weights of the  $L_3$  and  $L_2$  excitations, high quality data with good statistics was taken, and fitted with pseudo-Voigt functions, as shown in Fig. 3. The fitting results are listed in Table 1. All peak intensities are normalized to that of the  $L_3$  peak of our sample Cu<sub>4</sub> with  $\sigma_{4,L3} = 1.00$ . Equation (1) connects these spectral weights to the Cu occupation on the Cu(1,2) site in sample Cu<sub>3</sub> (Cu<sub>4</sub>),  $\rho_{3(4)}^{1(2)}$ , through the following relations:

$$\sigma_{4,L3} = (\rho_4^1 |\hat{M}_{L3}^1|^2 + \rho_4^2 |\hat{M}_{L3}^2|^2) \cdot C, \quad (2a)$$

$$\sigma_{4,L2} = (\rho_4^1 |\hat{M}_{L2}^1|^2 + \rho_4^2 |\hat{M}_{L2}^2|^2) \cdot C, \quad (2b)$$

$$\sigma_{3,L3} = (\rho_3^1 |\hat{M}_{L3}^1|^2 + \rho_3^2 |\hat{M}_{L3}^2|^2) \cdot C, \quad (2c)$$

$$\sigma_{3,L2} = (\rho_3^1 |\hat{M}_{L2}^1|^2 + \rho_3^2 |\hat{M}_{L2}^2|^2) \cdot C, \quad (2d)$$

where  $\hat{M}_{L_n}^m$  is the photon absorption matrix element in Eq. (1) for Cu( $m$ ) site at the  $L_n$  edge, and  $C$  is a scaling constant.

**Table 1.** Fitting results of  $L_3$  and  $L_2$  peaks.  $\sigma_{m,L_n}$  are the integrated intensities of the  $L_n$  peak for Cu <sub>$m$</sub>  samples. FWHM is the full width at half maximum of the peaks.

Peaks	Intensity (normalized)	FWHM (eV)	Center (eV)
Cu <sub>4</sub> $L_3$	$\sigma_{4,L3} = 1.00$	$1.45 \pm 0.01$	928.6
Cu <sub>4</sub> $L_2$	$\sigma_{4,L2} = 0.40 \pm 0.02$	$1.71 \pm 0.06$	948.4
Cu <sub>3</sub> $L_3$	$\sigma_{3,L3} = 0.68 \pm 0.01$	$1.35 \pm 0.01$	928.6
Cu <sub>3</sub> $L_2$	$\sigma_{3,L2} = 0.30 \pm 0.02$	$1.68 \pm 0.07$	948.4

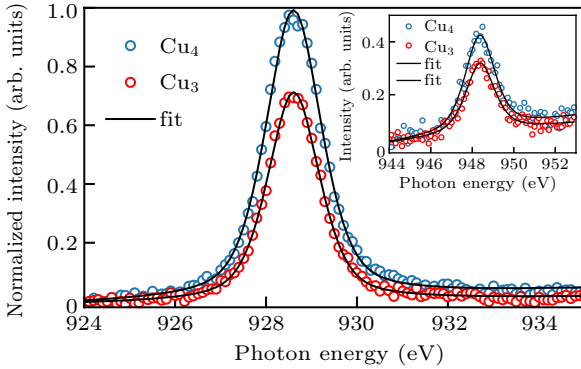


**Fig. 3.** Fitting of the spectra. Enlarged and averaged Cu  $L_3$ -edge XAS spectra of Cu<sub>4</sub> (blue circle) and Cu<sub>3</sub> (red circle) samples. The black lines represent the fitting curves. Both spectra are fitted by a pseudo-Voigt function and a linear background contribution. Inset shows the similar fitting for Cu  $L_2$ -edge peaks. In all of the fitting, least-squares method was used.

We take the following two steps to reduce the numbers of the unknown parameters. Firstly, we assume Cu<sub>4</sub> sample occupation ratios  $\rho_4^1/\rho_4^2 = 3 : 1$ . Secondly, we use the MultiX package<sup>[36]</sup> to evaluate the ratio among  $|\hat{M}_{L_n}^m|^2$ . The MultiX package was developed for core spectroscopies, based on multiplet analysis from a Dirac density functional atomic calculation. The calculation fully considers the real crystal structure and the Coulomb, spin-orbit, and crystal field interactions. The crystal structure as input parameters were taken

from Ref. [28]. For Cu<sup>2+</sup> configuration with one hole in the 3d shell, the XAS signal is insensitive to the on-site Coulomb interactions. The wavefunctions of the holes are determined by the crystal field environments and the relative strength of spin-orbit coupling (SOC) and the crystal field (CF). Thus there is only one tunable parameter, SOC/CF, to match the MultiX simulation to our data to extract the ratio of  $|\hat{M}_{L_n}^m|^2$  (see Table 2).

**Table 2.** The calculated photon absorption matrix elements. All the values are normalized to  $|\hat{M}_{L3}^2|^2$ .

$L_3$	$L_2$
$ \hat{M}_{L3}^1 ^2 = 0.797$	$ \hat{M}_{L2}^1 ^2 = 0.388$
$ \hat{M}_{L3}^2 ^2 = 1.000$	$ \hat{M}_{L2}^2 ^2 = 0.193$

Figure 4 shows the simulated XAS signals from Cu(1) (dashed blue line) and Cu(2) (solid pink line) sites. With the assumption that  $\rho_4^1/\rho_4^2 = 3 : 1$  in Cu<sub>4</sub> sample, the weighted summation (solid red line) of the contributions from the two sites is compared to our experimental data. The good agreement suggests that our extracted  $|\hat{M}_{L_n}^m|^2$  values are of high confidence.

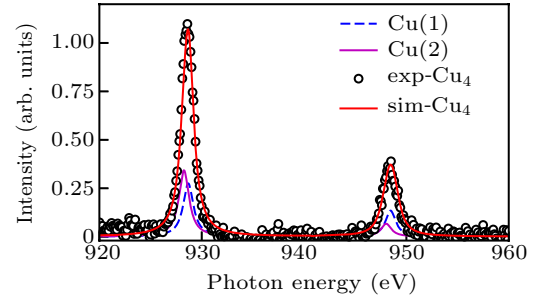


**Fig. 4.** Simulation of the whole spectra of Cu<sub>4</sub>(OH)<sub>6</sub>FBr. The TEY data of Cu<sub>4</sub>(OH)<sub>6</sub>FBr is overlapped with the simulated result from MultiX. The red line is the weighted sum of the simulated results of Cu(1) and Cu(2) sites (see text).

Clearly, the absorption matrix elements are drastically different between the Cu(1) and Cu(2) sites at the two  $L$ -edges. From the crystal structure (shown in Fig. 1), the Cu<sup>2+</sup> ions lie in two highly different local environments. Cu(1) is in kagomé plane, surrounded by four oxygen atoms and two bromine atoms, forming an octahedral crystal field environment. While Cu(2) is in inter-kagomé plane, whose nearest neighboring six oxygen atoms form a triangular prism. Thus strong contrast is expected in the transition matrix element  $\hat{M}_{if}$  for these two sites due to different crystal field effects.<sup>[36,42]</sup>

With the assumption that  $\rho_4^1/\rho_4^2 = 3 : 1$  and  $|\hat{M}_{L_n}^m|^2$  obtained (Table 2), equation (2) is reduced to the following:

$$\frac{\sigma_{4,L3}}{\sigma_{3,L3}} = \frac{3 \cdot 0.797 + 1 \cdot 1}{\rho_3^1 \cdot 0.797 + \rho_3^2 \cdot 1} = 1.47, \quad (3a)$$

$$\frac{\sigma_{4,L2}}{\sigma_{3,L2}} = \frac{3 \cdot 0.388 + 1 \cdot 0.193}{\rho_3^1 \cdot 0.388 + \rho_3^2 \cdot 0.193} = 1.32, \quad (3b)$$

where the ratios are from the fits of our XAS data. As a result, the Cu occupations on the Cu(1) and Cu(2) sites in Cu<sub>3</sub>

sample,  $\rho_3^1$  and  $\rho_3^2$  are deduced to be 2.469 and 0.335, respectively. These results suggest that, in our measured nominal  $\text{Cu}_3\text{Zn}(\text{OH})_6\text{FBr}$  sample, the inter-kagomé metal element site is 33.5% occupied by residual  $\text{Cu}^{2+}$ , while about 17.7% of the in-plane Cu(1) site is either vacant or occupied by Zn. The total count of Cu adds up to 2.805, close to nominal value 3.

#### 4. Discussion

Our results demonstrate the presence of significant antisite disorder in our measured nominal  $\text{Cu}_3\text{Zn}(\text{OH})_6\text{FBr}$  sample. Assuming no vacancies, our analysis suggests that the chemical formula of our sample is  $(\text{Cu}_{0.823}\text{Zn}_{0.177})_3(\text{Cu}_{0.335}\text{Zn}_{0.665})(\text{OH})_6\text{FBr}$ . It is helpful to compare these results with earlier measurements with other techniques. With ICP-OES measurements,<sup>[1,28,43]</sup> both Zn rich and Zn insufficient results were reported, and the degree of deviation from the ideal composition was suggested to be about 10%. However, ICP-OES only provides the total concentration of the elements rather than the site-specific content. Thus, the antisite disorder information is lost in ICP-OES results.

Another x-ray technique, namely, x-ray anomalous scattering, has been employed to determine the chemical disorder at different sites in herbertsmithite  $\text{Cu}_3\text{Zn}(\text{OH})_6\text{Cl}_2$ .<sup>[20]</sup> Their results suggested a nearly perfect Cu occupation in the kagomé layer while the inter-layer site was mixed with Zn:Cu = 0.85:0.15. In their analysis, the experimental results were compared to the calculated standard scattering factors for isolated Zn and Cu ions to extract the degree of Zn–Cu mixing on each site. These standard values from Hatree–Fock modeling with free atom approximation<sup>[34]</sup> may not be accurate for real materials since the anomalous scattering factors might vary in the specific chemical environments.<sup>[41]</sup>

The *L*-edge x-ray core-hole spectroscopy for  $\text{Cu}^{2+}$  has the well-defined  $2p \rightarrow 3d$  transition channel with only one unoccupied valence state. It can disentangle different local sites since the XAS feature depends on the local environment of the absorbing atoms.<sup>[44]</sup> Potentially it could be a good tool to determine the Cu concentration in  $\text{Cu}_3\text{Zn}(\text{OH})_6\text{FBr}$ . We explored such possibility. As discussed in the main text, our analysis heavily depends on the output of the MultiX package. Although MultiX takes real crystal structure, it is a simplified multiplet calculation with ionic model. Thus certain error is expected.

#### 5. Conclusion

Combining the Cu *L*-edge XAS measurements and the multiplet calculation with MultiX package,<sup>[36]</sup> we investigated the antisite mixing in the suggested spin-liquid system  $\text{Cu}_3\text{Zn}(\text{OH})_6\text{FBr}$ . Our results suggest that, in our measured

nominal  $\text{Cu}_3\text{Zn}(\text{OH})_6\text{FBr}$  sample, the inter-kagomé metal element site is 33.5% occupied by residual  $\text{Cu}^{2+}$ , while about 17.7% of the in-plane Cu(1) site is either vacant or occupied by Zn. In a related compound, the herbertsmithite, it has been shown that since  $\text{Zn}^{2+}$  and  $\text{Cu}^{2+}$  are similar in size,  $\text{Zn}^{2+}$  may occupies  $\text{Cu}^{2+}$  site in the kagome plane, leading to imperfect kagome plane.<sup>[45,46]</sup> Our results suggest that similar Zn intrusion into the kagome plane might also happen in  $\text{Cu}_3\text{Zn}(\text{OH})_6\text{FBr}$ .

The accurate determination of element concentration in materials with site sensitivities is generally difficult.  $\text{Cu}_3\text{Zn}(\text{OH})_6\text{FBr}$  and  $\text{Cu}_4(\text{OH})_6\text{FBr}$  serve as special cases where both Cu(1) and Cu(2) sites are of the same valence, and Zn and Cu are of similar ionic sizes. Our approach and the x-ray anomalous scattering analysis<sup>[20]</sup> could be complementary to each other.

#### References

- [1] Feng Z, Li Z, Meng X, Yi W, Wei Y, Zhang J, Wang Y C, Jiang W, Liu Z, Li S Y, Liu F, Luo J L, Li S L, Zheng G Q, Meng Z Y, Mei J W and Shi Y G 2017 *Chin. Phys. Lett.* **34** 077502
- [2] Anderson P W 1987 *Science* **235** 1196
- [3] Balents L 2010 *Nature* **464** 199
- [4] Kitaev A Y 2003 *Ann. Phys.* **303** 2
- [5] Liu X, Berlijn T, Yin W G, Ku W, Tsvelik A, Kim Y J, Gretarsson H, Singh Y, Gegenwart P and Hill J P 2011 *Phys. Rev. B* **83** 220403(R)
- [6] Broholm C, Cava R J, Kivelson S A, Nocera D G, Norman M R and Senthil T 2020 *Science* **367** eaay0668
- [7] Ran Y, Hermele M, Lee P A and Wen X G 2007 *Phys. Rev. Lett.* **98** 117205
- [8] Lawler M J, Paramakanti A, Kim Y B and Balents L 2008 *Phys. Rev. Lett.* **101** 197202
- [9] Sachdev S 1992 *Phys. Rev. B* **45** 12377
- [10] Norman M R 2016 *Rev. Mod. Phys.* **88** 041002
- [11] Helton J S, Matan K, Shores M P, Nytko E A, Bartlett B M, Yoshida Y, Takano Y, Suslov A, Qiu Y, Chung J H, Nocera D G and Lee Y S 2007 *Phys. Rev. Lett.* **98** 107204
- [12] Mendels P, Bert F, de Vries M A, Olariu A, Harrison A, Duc F, Trombe J C, Lord J S, Amato A and Baines C 2007 *Phys. Rev. Lett.* **98** 077204
- [13] Zorko A, Nellutla S, J van Tol, Brunel L C, Bert F, Duc F, Trombe J C, M A de Vries, Harrison A and Mendels P 2008 *Phys. Rev. Lett.* **101** 026405
- [14] Imai T, Nytko E A, Bartlett B M, Shores M P and Nocera D G 2008 *Phys. Rev. Lett.* **100** 077203
- [15] Fu M, Imai T, Han T H and Lee Y S 2015 *Science* **350** 655
- [16] Elliot P and Cooper M 2010 *Mineral. Mag.* **74** 797
- [17] Jeschke H O, Salvat-Pujol F, Gati E, Hoang N H, Wolf B, Lang M, Schlueter J A and Valent R 2015 *Phys. Rev. B* **92** 094417
- [18] Liu Z, Zou X, Mei J W and Liu F 2015 *Phys. Rev. B* **92** 220102
- [19] Smaha R W, He W, Sheckelton J P, Wen J and Lee Y S 2018 *J. Solid State Chem.* **268** 123
- [20] Freedman D E, Han T H, Prodi A, Müller P, Huang Q Z, Chen Y S, Webb S M, Lee Y S, McQueen T M and Nocera D G 2010 *J. Am. Chem. Soc.* **132** 16185
- [21] Smaha R W, Boukahil I, Titus C J, Jiang J M, Sheckelton J P, He W, Wen J, Vinson J, Wang S G, Chen Y S, Teat S J, Devereaux T P, Pemmarraju C D and Lee Y S 2020 *Phys. Rev. Materials* **4** 124406
- [22] Shores M P, Nytko E A, Bartlett B M and Nocera D G 2005 *J. Am. Chem. Soc.* **127** 13462
- [23] Han T H, Helton J S, Chu S Y, Nocera D G, Rodriguez-Rivera J A, Broholm C and Lee Y S 2012 *Nature* **492** 406
- [24] Han T H, Helton J S, Chu S, Prodi A, Singh D K, Mazzoli C, Müller P, Nocera D G and Lee Y S 2011 *Phys. Rev. B* **83** 100402
- [25] Asaba T, Han T H, Lawson B J, Yu F, Tinsman C, Xiang Z, Li G, Lee Y S and Li L 2014 *Phys. Rev. B* **90** 064417
- [26] Han T H, Norman M R, Wen J J, Rodriguez-Rivera J A, Helton J S, Broholm C and Lee Y S 2016 *Phys. Rev. B* **94** 060409



- [27] Olariu A, Mendels P, Bert F, Duc F, Trombe J C, M A de Vries and Harrison A 2008 *Phys. Rev. Lett.* **100** 087202
- [28] Feng Z, Wei Y, Liu R, Yan D, Wang Y C, Luo J L, Senyshyn A, Cruz C, Yi W, Mei J W, Meng Z Y, Shi Y and Li S L 2018 *Phys. Rev. B* **98** 155127
- [29] Smaha R W, He W, Jiang J M, Wen J J, Jiang Y F, Sheckelton J P, Titus C J, Wang S G, Chen Y S, Teat S J, Aczel A A, Zhao Y, Xu G, Lynn J W, Jiang H C and Lee Y S 2020 *npj Quantum Mater.* **5** 23
- [30] Tustain K, Ward-O'Brien B, Bert F, Han T H, Luetkens H, Lancaster T, Huddart B M, Baker P J and Clark L 2020 *npj Quantum Mater.* **5** 74
- [31] Han T H, Singleton J and Schlueter J A 2014 *Phys. Rev. Lett.* **113** 227203
- [32] Lee H C 2018 *Appl. Phys. Rev.* **5** 011108
- [33] Frankel R S and Aitken D W 1970 *Applied Spectroscopy* **24** 557
- [34] Cromer D T and Mann J B 1968 *Acta Crystallogr. A* **24** 321
- [35] Fink J, Heinzerling M, Scheerer B, Speier W, Hillebrecht F U, Fuggle J C, Zaanen J and Sawatzky G A 1985 *Phys. Rev. B* **32** 4899
- [36] Uldry A, Vernay F and Delley B 2012 *Phys. Rev. B* **85** 125133
- [37] de Groot F and Kotani A 2008 *Core Level Spectroscopy of Solids*
- [38] Meyers D, Mukherjee S, Cheng J G, Middey S, Zhou J S, Goodenough J B, Gray B A, Freeland J W, Saha-Dasgupta T and Chakhalian J 2013 *Sci. Rep.* **3** 1834
- [39] Huang S W, Wray L A, Jeng H T, Tra V T, Lee J M, Langner M C, Chen J M, Roy S, Chu Y H, Schoenlein R W, Chuang Y D and Lin J Y 2015 *Sci. Rep.* **5** 16690
- [40] de Groot F M F 1995 *Physica B* **208–209** 15
- [41] Als-Nielsen J and McMorrow D 2001 *Elements of Modern X-ray Physics* (New York: John Wiley and Sons) p. 186
- [42] Haverkort M W, Zwierzycki M and Andersen O K 2012 *Phys. Rev. B* **85** 165113
- [43] Wei Y, Feng Z, Lohstroh W, *et al.* 2017 arXiv:1710.02991 [cond-mat.str-el]
- [44] Magnuson M, Schmitt T, Strocov V, Schlappa J, Kalabukhov A S and Duda L C 2014 *Sci. Rep.* **4** 7017
- [45] Lee S H, Kikuchi H, Qiu Y, Lake B, Huang Q, Habicht K and Kiefer K 2007 *Nature Mater.* **6** 853
- [46] Bert F, Nakamae S, Ladieu F, L'Hôte D, Bonville P, Duc F, Trombe J C and Mendels P 2007 *Phys. Rev. B* **76** 132411